Disruption of Insulin Receptor Substrate 2 Causes Type 2 Diabetes Because of Liver Insulin Resistance and Lack of Compensatory β-Cell Hyperplasia

Naoto Kubota, Kazuyuki Tobe, Yasuo Terauchi, Kazuhiro Eto, Toshimasa Yamauchi, Ryo Suzuki, Yoshiharu Tsubamoto, Kajuro Komeda, Ryosuke Nakano, Hiroshi Miki, Shinobu Satoh, Hisahiko Sekihara, Salvatore Sciacchitano, Maxine Lesniak, Shinichi Aizawa, Ryozo Nagai, Satoshi Kimura, Yasuo Akanuma, Simeon I. Taylor, and Takashi Kadowaki

To investigate the role of insulin receptor substrate (IRS)-2 in vivo, we generated IRS-2–deficient mice by gene targeting. Although homozygous IRS-2–deficient mice (*IRS-2*$^{-/-}$ mice) had a body weight similar to wild-type mice, they progressively developed type 2 diabetes at 10 weeks. *IRS-2*$^{-/-}$ mice showed insulin resistance and a defect in the insulin-stimulated signaling pathway in liver but not in skeletal muscle. Despite insulin resistance, the amount of β-cells was reduced to 83% of that in wild-type mice, which was in marked contrast to the 85% increase in the amount of β-cells in IRS-1–deficient mice (*IRS-1*$^{-/-}$ mice) to compensate for insulin resistance. Thus, IRS-2 plays a crucial role in the regulation of β-cell mass. On the other hand, insulin secretion by the same number of cells in response to glucose measured ex vivo was significantly increased in *IRS-2*$^{-/-}$ mice compared with wild-type mice but was decreased in *IRS-1*$^{-/-}$ mice. These results suggest that IRS-1 and IRS-2 may play different roles in the regulation of β-cell mass and the function of individual β-cells. *Diabetes* 49:1880–1889, 2000

The pathogenesis of type 2 diabetes involves complex interactions among multiple physiological defects. Transgenic and knockout technology used to create animal models of type 2 diabetes have had a major impact on assessment of the function of newly identified molecules implicated in the regulation of glucose homeostasis in vivo (1). Insulin receptor substrate (IRS)-1 was originally identified as the major substrate of insulin receptor and IGF-1 receptor tyrosine kinases (2–4) and represents the prototype of the IRS family proteins (5–7). To clarify the physiological roles of IRS-1 in vivo, we (8) and others (9) produced mice with a targeted disruption of the IRS-1 gene locus. Homozygous IRS-1–deficient mice (*IRS-1*$^{-/-}$ mice) were born alive but were retarded in embryonal and postnatal growth (8,9), indicating that IRS-1 is indispensable for the growth-promoting function of insulin and IGF. They also had resistance to the glucose-lowering effects of insulin and IGF. Nevertheless, *IRS-1*$^{-/-}$ mice maintained normal fasting glucose and glucose tolerance by compensatory β-cell hyperplasia (8,10). These data suggest the existence of both IRS-1–dependent and IRS-1–independent pathways for signal transduction of insulin and IGF (8,9). Kahn's group (Araki et al. [9] and Patti et al. [11]) identified an alternate substrate in the liver in *IRS-1*$^{-/-}$ mice, which they subsequently identified as IRS-2. We also identified a 190-kDa protein (pp190) in the liver of *IRS-1*$^{-/-}$ mice, of which tyrosine phosphorylation was robustly stimulated by insulin (12). Like IRS-1, pp190 was capable of binding both the 85-kDa subunit of phosphatidylinositol (PI) 3-kinase and the Grb2 molecule (12). Interestingly, the amount of tyrosine phosphorylation of IRS-2 (pp190) in the liver of *IRS-1*$^{-/-}$ mice was equivalent to that of IRS-1 in the liver of wild-type mice and appeared to fully compensate for IRS-1 in insulin actions (13). Insulin-stimulated PI 3-kinase activation was normal in the liver of *IRS-1*$^{-/-}$ mice but was defective in the skeletal muscle of *IRS-1*$^{-/-}$ mice, presumably because of significantly reduced tyrosine phosphorylation of IRS-2 compared with IRS-1 in wild-type mice (13). We and others thus suggested that IRS-2 may play an important role in insulin action, particularly in the liver (13,14).

To investigate the role of IRS-2 in vivo, we generated IRS-2–deficient mice by gene targeting. The phenotype of these mice was strikingly different from that of *IRS-1*$^{-/-}$ mice. Although homozygous IRS-2–deficient mice (*IRS-2*$^{-/-}$ mice) were normal in size, they progressively developed type 2 diabetes at 10 weeks. *IRS-2*$^{-/-}$ mice were already insulin resistant at 6 weeks, presumably because of insulin resistance in the liver but not in the skeletal muscle. Despite insulin resistance, the amount of β-cells was reduced to 83% of that of wild-type mice, which was in marked contrast to the 85% increase in the amount of β-cells in *IRS-1*$^{-/-}$ mice at 6 weeks. Thus, liver insulin resistance together with a lack of com-

From the Department of Metabolic Diseases (N.K., K.T., Y.Te., K.E., T.Y., R.S., Y.Ts., R.Nak., H.M., R.Nag., S.K., T.K.), Graduate School of Medicine, University of Tokyo; the Division of Laboratory Animal Science (K.K.), Animal Research Center, Tokyo Medical University, Tokyo; the Third Department of Internal Medicine (S.Sa., H.S.), Yokohama City University, Yokohama; Institute for Diabetes Care and Research (Y.A.), Asahi Life Foundation; the Department of Morphogenesis (S.A.), Institute of Molecular Embryology and Genetics, Kumamoto University School of Medicine, Kumamoto, Japan; and the Diabetes Branch (S.Sc., M.L., S.I.T.), National Institute of Diabetes and Digestive Diseases, National Institutes of Health, Bethesda, Maryland.

Address correspondence and reprint requests to Takashi Kadowaki, MD, PhD, Department of Metabolic Diseases, Graduate School of Medicine, University of Tokyo, 7-3-1 Hongo, Bunkyo-ku, Tokyo 113-8655, Japan. E-mail: kadowaki-3im@h.u-tokyo.ac.jp.

Received for publication 29 December 1999 and accepted in revised form 14 July 2000.

K.T., Y.Te., and K.E. contributed equally to this work.

H.M. is employed by Takeda Chemical Industries, Osaka, Japan.

IRS, insulin receptor substrate; PI, phosphatidylinositol; PY, phosphotyrosine; RIA, radioimmunoassay.

pensatory β-cell hyperplasia caused type 2 diabetes in *IRS-2*$^{-/-}$ mice. These results were qualitatively similar to those previously reported by Withers et al. (15). However, the degree of hyperglycemia was milder in our *IRS-2*$^{-/-}$ mice than their *IRS-2*$^{-/-}$ mice. Moreover, we report here that insulin secretion in response to glucose from the same number of cells measured ex vivo was significantly increased in *IRS-2*$^{-/-}$ mice but decreased in *IRS-1*$^{-/-}$ mice compared with wild-type mice. These results suggest that IRS-1 and IRS-2 may play different roles in the regulation of β-cell mass and function of individual β-cells.

RESEARCH DESIGN AND METHODS

Construction of the targeting vector. To construct the targeting vector for disruption of the IRS-2 gene, a Balb/c mouse genomic DNA library, packaged in EMBL3 (Clontech, Palo Alto, CA), was screened using a 400-bp polymerase chain reaction product of mouse IRS-2 as a probe. Three clones containing the IRS-2 gene were isolated. To inactivate the IRS-2 gene, a neomycin-resistant gene (*neoR*) with a pgk-1 promoter and with no poly (A)$^+$ addition signal was inserted into the *Stu*I site. The presence of several stop codons in the pgk-1 promoter was expected to destabilize IRS-2 mRNA. The diphtheria toxin A fragment (DTA) gene under an MC1 promoter was ligated onto the 3′ end of the homologous region for negative selection against random integration (16).

Embryonic stem cell culture and generation of mutant mice. The strategy for culturing and electroporation of TT2 embryonic stem cells (C57Bl/6 × CBA) and screening of homologous recombinant clones was as described previously (16,17). These cells were injected into eight-cell embryos from ICR mice (albino coat color) and transferred into pseudopregnant ICR females to generate chimeric mice. Male chimeras with black coat color were mated with C57Bl/6J female mice to generate heterozygous and homozygous offspring. Thus, knockout animals were maintained on a mixed C57Bl/6 × CBA genetic background.

Animals. *IRS-1*$^{-/-}$ mice (8) and *IRS-2*$^{-/-}$ mice were maintained on the original C57B1/6 × CBA hybrid background. *IRS-1*$^{-/-}$ mice and wild-type mice were prepared by *IRS-1*$^{+/-}$ mice intercrosses, and *IRS-2*$^{-/-}$ mice and wild-type mice were prepared by *IRS-2*$^{+/-}$ mice intercrosses. All mice were maintained on a 12-h/12-h light/dark cycle. All experiments in this study were performed using male mice, except for the experiments in which female mice were analyzed.

RNA preparation and Northern blot analysis. Total RNA was prepared from liver with TRIzol Reagent Total RNA isolation reagent (Gibco, Rockville, MD) according to the manufacturer's instructions. Northern blot analysis was performed according to the standard protocol using 30 μg total RNA. In brief, total RNA from liver was loaded onto a 1.0% agarose gel containing 5.5% formaldehyde in 1× MOPS buffer (0.4 mol/l MOPS, 100 mmol/l sodium acetate, 200 mmol/l EDTA) and was transferred to Hybond-N$^+$ (Amersham Pharmacia Biotech, Buckinghamshire, U.K.). After ultraviolet cross-linking, the membrane was hybridized with digoxigenin-11-UTP–labeled probe overnight in a hybridization buffer (Ambion, Austin, TX) at 68°C and washed twice at 15 min in 0.1 × sodium chloride–sodium citrate/0.1% SDS at 68°C before exposing to X-ray film.

PI 3-kinase assay in liver and skeletal muscle. PI 3-kinase activities in the liver and skeletal muscles were determined in immunoprecipitates with the indicated antibody after 400 μg insulin per mouse was injected into the posterior vena cava. The liver and skeletal muscles were removed at 70 s and 2 min, respectively, after the injection. PI 3–kinase activity was measured in the immunoprecipitates with antibody against a COOH-terminal peptide of IRS-1 (anti–IRS-1; Upstate Biotechnology, NY), antibody against an NH_2-terminal portion of IRS-2 (anti–IRS-2; Santa Cruz Technology, Santa Cruz, CA), and antibody against a phosphotyrosine (anti-PY; UBI), and its activity was measured as described (13). The amounts of PI 3–kinase activity were quantitated with an image analyzer (BAS 2000; Fuji Film, Tokyo) and expressed as the intensity of phospho-stimulated luminescence.

Immunoblotting. Tissues were excised and homogenized in ice-cold buffer A (25 mmol/l Tris-HCl, pH 7.4, 10 mmol/l sodium orthovanadate, 10 mmol/l sodium pyrophosphate, 100 mmol/l sodium fluoride, 10 mmol/l EDTA, 10 mmol/l EGTA, and 1 mmol/l phenylmethylsulfonyl fluoride). Samples were separated on 7% polyacrylamide gels and transferred to nitrocellulose. Immunoprecipitation of liver and skeletal muscle proteins was as described previously (13).

In vivo glucose homeostasis

Glucose tolerance test. Mice were fasted for >16 h before the study. They were then loaded with 1.5 mg/g body wt glucose by oral administration. Blood samples were taken at different time points from the orbital sinus, and glucose was measured using an automatic blood glucose meter (Glutest Ace; Sanwa Chemical, Nagoya, Japan). Whole blood was collected and centrifuged in heparinized tubes, and the plasma was stored at –20°C. Insulin levels were determined using an insulin radioimmunoassay (RIA) kit (BIOTRAK; Amersham Pharmacia Biotech) with rat insulin as a standard (18).

Insulin tolerance test. Mice were fed freely and then fasted during the study. They were intraperitoneally challenged with 0.75 mU/g body wt human insulin (Novolin R; Novo Nordisk, Denmark). Blood samples were drawn from the vein at different time points (19).

Histological and immunohistochemical analysis of islets. Four male mice at 6 and 12 weeks were used for each genotype, and 20 sections of islets were evaluated for morphometry. The isolated pancreases were immersion-fixed in Bouin's solution at 4°C overnight. Tissues were routinely processed for paraffin embedding, and 4-μm sections were cut and mounted on silanized slides. Pancreatic sections were double-stained with anti-insulin and cocktails of anti-glucagon, anti-somatostatin, and anti-pancreatic polypeptide antibodies. Images of pancreatic tissue, islet β-cells, and islet non–β-cells were viewed on the monitor of a computer through a microscope connected to a charged coupling device camera (Olympus, Tokyo), as previously described (10). The areas of pancreases, β-cells, and non–β-cells were traced manually and analyzed with Win ROOF software (Mitani, Chiba, Japan). The amounts of β-cells and non–β-cells were calculated as the proportions of the area of β-cells or non–β-cells, assessed by immunostaining, to the area of the whole pancreas (10,20). More than 50 islets were analyzed per mouse in each group.

Islet isolation and β-cell preparation. Isolation of islets from *IRS-1*$^{-/-}$ mice, *IRS-2*$^{-/-}$ mice, and their wild-type litter mates was carried out as described previously (21). In brief, after clamping the common bile duct at a point close to the duodenum outlet, 2.5 ml Krebs-Ringer bicarbonate buffer (129 mmol/l NaCl, 4.8 mmol/l KCl, 1.2 mmol/l $MgSO_4$, 1.2 mmol/l KH_2PO_4, 2.5 mmol/l $CaCl_2$, 5 mmol/l $NaHCO_3$, and 10 mmol/l HEPES at pH 7.4) containing collagenase (Sigma, St. Louis, MO) was injected into the duct. The swollen pancreas was taken out and incubated at 37°C for 3 min. The pancreas was dispersed by pipetting and washed two times with Krebs-Ringer bicarbonate buffer. Islets were collected by manual picking. Single cells were isolated with Trypsin-EDTA (Gibco) as previously described (22) with some modification.

Analysis of insulin content and secretion. Isolated islets were extracted in acid ethanol at –20°C, and their insulin content was measured by RIA. Insulin secretion by islets was measured with Krebs-Ringer bicarbonate buffer with a basal glucose concentration of 2.8 mmol/l, unless otherwise stated. Static incubation was performed with 10 islets per tube at 37°C for 1 h after preincubation with the basal glucose concentration for 20 min (21,22). Insulin levels were determined with an insulin RIA kit (BIOTRAK) with rat insulin as the standard (18). The number of islet cells was measured with a hemacytometer.

RESULTS

Disruption of the IRS-2 gene in mice. *IRS-2*$^{-/-}$ mice were generated by homologous recombination (Fig. 1*A*). The male chimeras that originated from the TT2 embryonic stem cells with the desired homologous integration transmitted the mutant IRS-2 allele to their offspring. Mice heterozygous for the mutation were viable and bred to generate homozygous mutants. We confirmed homologous recombination by Southern blot analysis (Fig. 1*B*). Northern blot analysis by using the 5′ probe to the *Stu*I site did not detect any expression of IRS-2 mRNA in *IRS-2*$^{-/-}$ mice but revealed an ~50% reduction in *IRS-2*$^{+/-}$ mice (Fig. 1*C*). Western blot analysis using an antibody against the COOH-terminus of IRS-2 confirmed that expression of IRS-2 was completely abrogated in *IRS-2*$^{-/-}$ mice (Fig. 1*D*). Western blot analysis to detect insulin-stimulated tyrosine phosphorylation of IRS-2 by immunoprecipitation with antibody against the NH_2-terminus of IRS-2 followed by blotting with anti-PY revealed that IRS-2 was tyrosine phosphorylated in wild-type mice but not in *IRS-2*$^{-/-}$ mice (Fig. 1*E*). Moreover, when lysates of liver and skeletal muscle from wild-type and *IRS-2*$^{-/-}$ mice were immunoprecipitated with anti-PY and blotted with anti-PY, no new tyrosine-phosphorylated protein with the approximate size expected for the NH_2-terminus fragment in *IRS-2*$^{-/-}$ mice was detected (Fig. 1*F*). In addition,

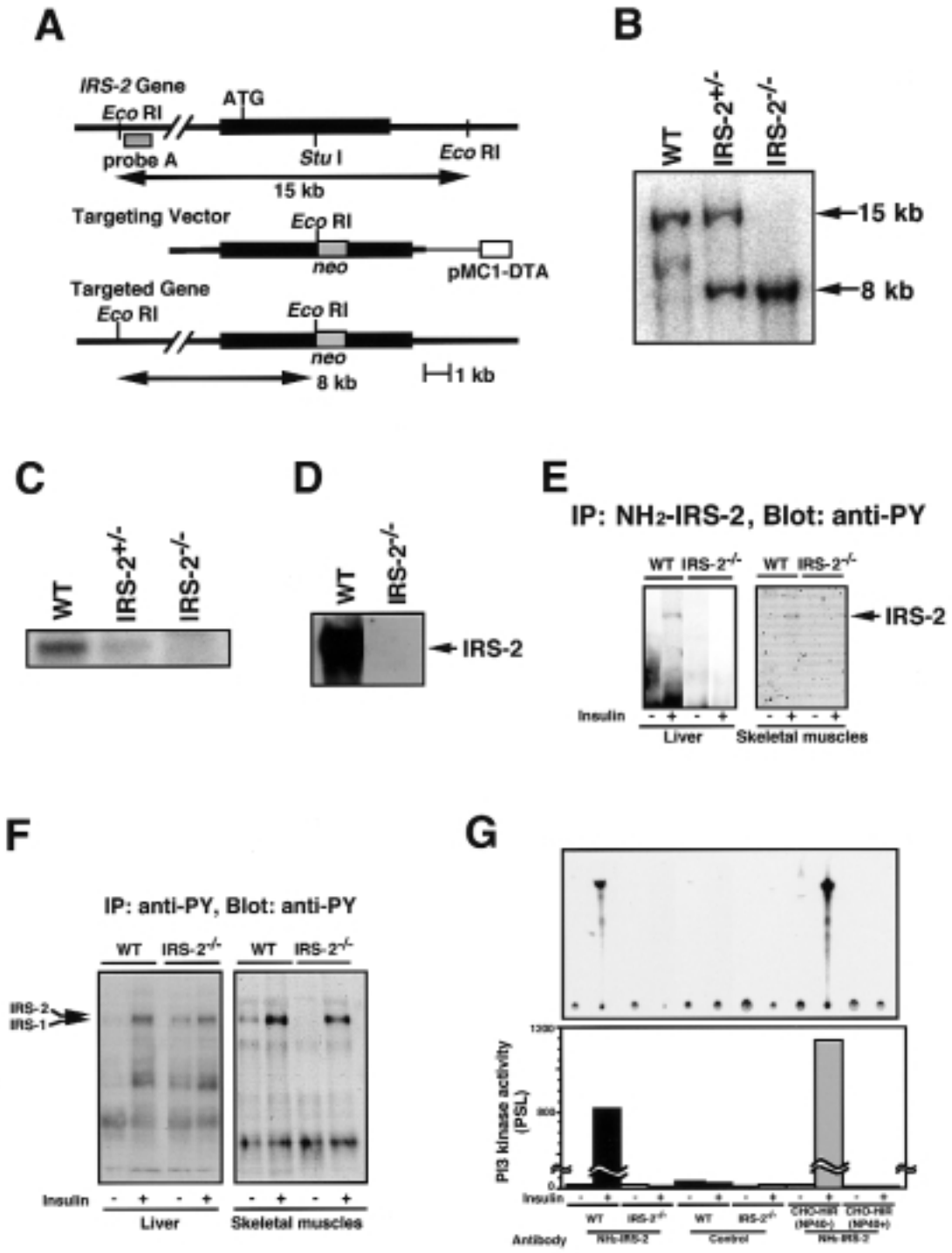

FIG. 1. Targeted disruption of the IRS-2 gene. *A*: Schematic representation of the gene targeting strategy. Top: Partial restriction map of the IRS-2 locus. Middle: IRS-2 gene targeting vector. Bottom: The expected mutant locus. The DNA fragment used as probe A for Southern blotting is also shown under the top figure. *B*: *Eco*RI-digested mouse genomic DNA from wild-type (WT), *IRS-2*$^{+/-}$, and *IRS-2*$^{-/-}$ mice hybridized with probe A. The 15-kb band corresponds to the wild-type allele and the 8-kb band to the mutant allele. *C*: Northern blot analysis of total RNA from the liver of each genotype. Expression of the IRS-2 gene was examined by using a 5′ antisense RNA probe to the *Stu*I site in IRS-2. Aliquots of total RNA (30 µg) were hybridized with the IRS-2 cRNA probe. Mouse G3PDH was used as the loading control (data not shown). *D*: Equal amounts (0.1 mg) of liver lysates from wild-type and *IRS-2*$^{-/-}$ mice were immunoprecipitated with anti–IRS-2 and blotted with anti–IRS-2. *E*: Insulin-stimulated tyrosine phosphorylation of IRS-2 in the liver. Equal amounts of protein (0.1 mg) from untreated and insulin-treated 6-week-old mice were immunoprecipitated (IP) with antibody against the NH_2-terminus of IRS-2 and blotted with anti-PY. *F*: Equal amounts (0.1 mg) of liver and skeletal muscle lysates from wild-type and *IRS-2*$^{-/-}$ mice were immunoprecipitated with anti-PY and blotted with anti-PY. *G*: Insulin-stimulated PI 3–kinase activity associated with IRS-2 in the liver from wild-type and *IRS-2*$^{-/-}$ mice. Equal amounts of protein (50 µg) from untreated and insulin-treated 6-week-old mice were immunoprecipitated with antibody against the NH_2-terminus of IRS-2; immunoprecipitates were assayed in vitro for PI 3–kinase activity. Control antibody was used as a negative control in this experiment, and Chinese hamster ovary cells overexpressing human insulin receptor (CHO-HIR) were used as a positive control. The upper panels show spots of phosphatidylinositol(3)phosphate. PI 3–kinase activity was quantitated with an image analyzer. PSL, phospho-stimulated luminescence. □, Wild-type mice; ■, *IRS-2*$^{-/-}$ mice; ▩, CHO-HIR.

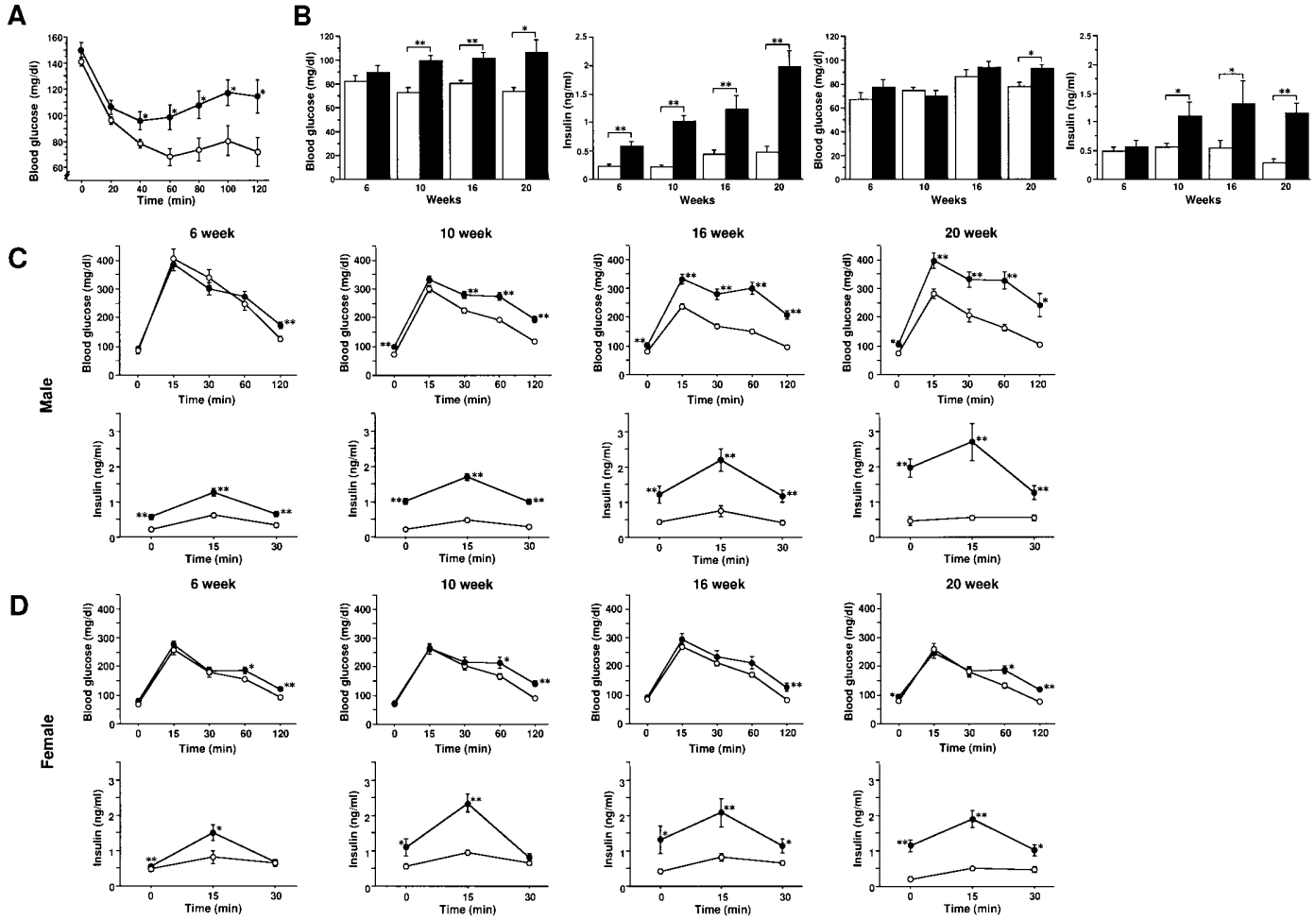

FIG. 2. *IRS-2*$^{-/-}$ mice showed insulin resistance and developed type 2 diabetes. *A*: Insulin tolerance test of wild-type and *IRS-2*$^{-/-}$ mice at 6 weeks. Mice were fed freely and then given 0.75 mU of human insulin per gram of body weight. Blood glucose levels were measured at the times indicated. Values are expressed as means ± SE obtained from the analysis of wild-type (○, *n* = 17) and *IRS-2*$^{-/-}$ mice (●, *n* = 21). **P* < 0.05. *B*: Time course of the fasting glucose and insulin levels of male and female wild-type and *IRS-2*$^{-/-}$ mice. Values are expressed as means ± SE obtained from the analysis of male wild-type mice (□, *n* = 13 at 6 weeks, *n* = 36 at 10 weeks, *n* = 15 at 16 weeks, and *n* = 8 at 20 weeks), male *IRS-2*$^{-/-}$ mice (■, *n* = 16 at 6 weeks, *n* = 47 at 10 weeks, *n* = 18 at 16 weeks, and *n* = 11 at 20 weeks), female wild-type mice (□, *n* = 11 at 6 weeks, *n* = 12 at 10 weeks, *n* = 12 at 16 weeks, and *n* = 6 at 20 weeks), and female *IRS-2*$^{-/-}$ mice (■, *n* = 12 at 6 weeks, *n* = 10 at 10 weeks, *n* = 11 at 16 weeks, and *n* = 12 at 20 weeks). **P* < 0.05; ***P* < 0.01. *C*: Oral glucose tolerance test results of male wild-type and *IRS-2*$^{-/-}$ mice at 6, 10, 16, and 20 weeks. Blood glucose (upper panel) and plasma insulin levels (lower panel) were measured at the times indicated. Values are expressed as means ± SE obtained from the analysis of wild-type mice (○, *n* = 13 at 6 weeks, *n* = 36 at 10 weeks, *n* = 15 at 16 weeks, and *n* = 8 at 20 weeks) and male *IRS-2*$^{-/-}$ mice (●, *n* = 16 at 6 weeks, *n* = 47 at 10 weeks, *n* = 18 at 16 weeks, and *n* = 11 at 20 weeks). **P* < 0.05; ***P* < 0.01. *D*: Oral glucose tolerance test of female wild-type and *IRS-2*$^{-/-}$ mice at 6, 10, 16, and 20 weeks. Blood glucose (upper panel) and plasma insulin levels (lower panel) were measured at the times indicated. Values are expressed as means ± SE obtained from the analysis of wild-type mice (○, *n* = 11 at 6 weeks, *n* = 12 at 10 weeks, *n* = 12 at 16 weeks, and *n* = 6 at 20 weeks) and female *IRS-2*$^{-/-}$ mice (●, *n* = 12 at 6 weeks, *n* = 10 at 10 weeks, *n* = 11 at 16 weeks, and *n* = 12 at 20 weeks). **P* < 0.05; ***P* < 0.01.

when lysates from liver were directly immunoprecipitated with antibody against the NH_2-terminus of IRS-2, no insulin-stimulated PI 3–kinase activity associated with IRS-2 was detected in *IRS-2*$^{-/-}$ mice (Fig. 1*G*).

***IRS-2*$^{-/-}$ mice showed insulin resistance and developed type 2 diabetes.** Unlike *IRS-1*$^{-/-}$ mice (8,9), *IRS-2*$^{-/-}$ mice had normal birth size and body weight (data not shown). Figure 2*A* shows the insulin tolerance of wild-type and *IRS-2*$^{-/-}$ mice at 6 weeks. The glucose-lowering effect of insulin was significantly impaired in *IRS-2*$^{-/-}$ mice compared with wild-type mice, suggesting that *IRS-2*$^{-/-}$ mice showed insulin resistance. We next performed an oral glucose tolerance test at 6, 10, 16, and 20 weeks for each sex of wild-type and *IRS-2*$^{-/-}$ mice. At 6 weeks, the blood glucose levels before and after the glucose load were not significantly different between the wild-type and *IRS-2*$^{-/-}$ mice (Fig. 2*B* and *C*). After 10 weeks, however, the blood glucose levels both before and after the glucose load gradually became higher in the *IRS-2*$^{-/-}$ mice compared with the wild-type mice (Fig. 2*B* and *C*). The curve of blood glucose levels of *IRS-2*$^{-/-}$ mice did not descend with age, whereas that of male wild-type mice did. Plasma insulin levels before and after the glucose load were already higher at 6 weeks in the *IRS-2*$^{-/-}$ mice than in the wild-type mice, indicating that the *IRS-2*$^{-/-}$ mice were insulin resistant. On the other hand, the female *IRS-2*$^{-/-}$ mice maintained minimally impaired glucose tolerance at 20 weeks (Fig. 2*B*). At 20 weeks, fasting plasma insulin levels were lower in the female *IRS-2*$^{-/-}$ mice than in the male *IRS-2*$^{-/-}$ mice (Fig. 2*B* and *D*).

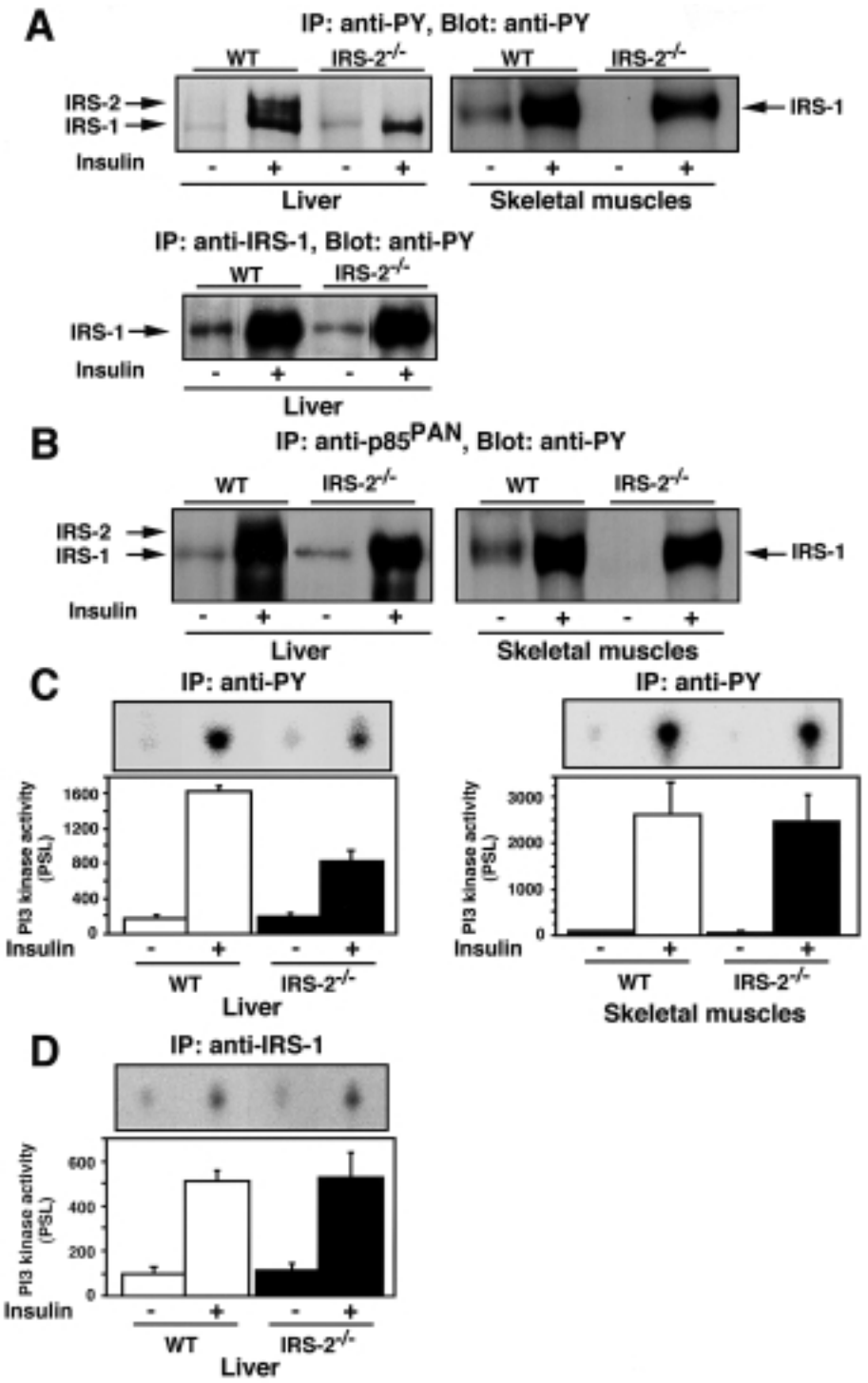

FIG. 3. Insulin-signaling pathways in the liver and skeletal muscle of *IRS-2*$^{-/-}$ mice. *A*: Upper panels: Insulin-stimulated tyrosine phosphorylation of IRS-1 and IRS-2 in liver (left) and skeletal muscle (right). Equal amounts of protein (0.1 mg) from untreated and insulin-treated 6-week-old mice were immunoprecipitated (IP) with anti-PY antibody and blotted for anti-PY. Lower panel: Insulin-stimulated tyrosine phosphorylation of IRS-1 in the liver. Equal amounts of protein (0.1 mg) from untreated and insulin-treated 6-week-old mice were immunoprecipitated with anti–IRS-1 antibody and blotted for anti-PY. WT, wild-type. *B*: Insulin-stimulated association of the p85α subunit of PI 3-kinase with insulin-stimulated tyrosine phosphorylated IRS-1 and IRS-2 in wild-type and *IRS-2*$^{-/-}$ mice. Equal amounts of protein (0.1 mg) from untreated and insulin-treated 6-week-old mice were immunoprecipitated with anti-p85^{PAN} antibody and blotted for anti-PY. *C*: Insulin-stimulated PI 3–kinase activity associated with insulin-stimulated tyrosine phosphorylated proteins in the liver and skeletal muscle of wild-type and *IRS-2*$^{-/-}$ mice. Equal amounts of protein (0.1 mg) from untreated and insulin-treated 6-week-old mice were immunoprecipitated with anti-PY antibody; immunoprecipitates were assayed in vitro for PI 3–kinase activity. The upper panels show spots of phosphatidylinositol(3)phosphate. The amounts of PI 3–kinase activity were quantitated with an image analyzer (BAS 2000) and expressed as the intensity of phospho-stimulated luminescence (PSL). Values are expressed as means ± SE (n = 5–6) (lower panels). □, Wild-type mice; ■, *IRS-2*$^{-/-}$. *D*: Insulin-stimulated PI 3–kinase activity associated with insulin-stimulated IRS-1 in the liver in wild-type mice and *IRS-2*$^{-/-}$ mice. Equal amounts of protein (0.1 mg) from untreated and insulin-treated 6-week-old mice were immunoprecipitated with anti–IRS-1 antibody; immunoprecipitates were assayed in vitro for PI 3–kinase activity. Values are expressed as means ± SE (n = 4) (lower panels).

Insulin-signaling pathways in the liver and skeletal muscle of *IRS-2*$^{-/-}$ mice. To investigate the biochemical basis for the observed insulin resistance in *IRS-2*$^{-/-}$ mice, we studied insulin-stimulated tyrosine phosphorylation of IRS-1 and IRS-2 by immunoprecipitation with anti-PY antibody in the liver and skeletal muscle of *IRS-2*$^{-/-}$ mice compared with wild-type mice. In the liver and skeletal muscle of *IRS-2*$^{-/-}$ mice, insulin failed to cause tyrosine phosphorylation of IRS-2 (Fig. 3*A*). However, in the liver and skeletal muscle of *IRS-2*$^{-/-}$ mice, insulin caused strong tyrosine phosphorylation of IRS-1 to a degree similar to that seen in wild-type mice (Fig. 3*A*). In fact, when lysates from liver were directly immunoprecipitated with anti–IRS-1 antibody, IRS-1 was tyrosine phosphorylated to a similar extent in both wild-type mice and *IRS-2*$^{-/-}$ mice (Fig. 3*A*). We next studied insulin-stimulated association of the p85α subunit of PI 3-kinase with insulin-stimulated tyrosine-phosphorylated proteins such as IRS-1 and IRS-2 in wild-type and *IRS-2*$^{-/-}$ mice. Consistent with the results of tyrosine phosphorylation of IRS-1 in *IRS-2*$^{-/-}$ mice, association of p85α with IRS-1 was normal in the liver and skeletal muscle of *IRS-2*$^{-/-}$ mice (Fig. 3*B*). Insulin-stimulated PI 3–kinase activity associated with insulin-stimulated tyrosine-phosphorylated proteins was significantly reduced in the liver but was normal in the skeletal muscle (Fig. 3*C*). However, when lysates from liver were directly immunoprecipitated with anti–IRS-1 antibody, insulin-stimulated PI 3–kinase activity associated with insulin-stimulated IRS-1 proteins was normal (Fig. 3*D*). These results suggest that the insulin resistance seen in *IRS-2*$^{-/-}$ mice is specific to liver because of loss of PI 3–kinase activity associated with IRS-2. These results are inconsistent with the original report of *IRS-2*$^{-/-}$ mice (15), in which it was argued that IRS-2 deficiency in the liver caused a defect of insulin-stimulated tyrosine phosphorylation of IRS-1 in addition to that of IRS-2.

Reduced β-cell mass in *IRS-2*$^{-/-}$ mice. Figure 4 shows the results of quantitative histological analysis of the pancreatic islets and quantitation of β-cell mass in wild-type, *IRS-1*$^{-/-}$, and *IRS-2*$^{-/-}$ mice. As we previously reported (10), at 6 and 12 weeks, the β-cell mass of *IRS-1*$^{-/-}$ mice was increased 85 and 95%, respectively, compared with that of wild-type mice. However, at 6 weeks, the β-cell mass of the *IRS-2*$^{-/-}$ mice was reduced to 83% of that of the wild-type mice. At 12 weeks, the β-cell mass of the *IRS-2*$^{-/-}$ mice was significantly reduced to 51% of that of the wild-type mice. This reduction was specific to β-cells, since the non–β-cell mass was similar between wild-type and *IRS-2*$^{-/-}$ mice (Fig. 4).

Normal insulin content and increased insulin secretion in *IRS-2*$^{-/-}$ mice. We determined glucose-induced insulin secretion in *IRS-2*$^{-/-}$ mice by static incubation of the same numbers of islets for 1 h. Whereas insulin secretion into the medium by islets from *IRS-2*$^{-/-}$ and wild-type mice was similar at 2.8, 5.6, and 11.1 mmol/l glucose, at 22.2 mmol/l glucose, insulin secretion by islets from *IRS-2*$^{-/-}$ mice increased slightly but significantly compared with islets from wild-type mice (Fig. 5*A*). When glucose-induced insulin secretion was normalized by cell number, secretion by *IRS-2*$^{-/-}$ islets was significantly higher at 11.1 and 22.2 mmol/l glucose than by wild-type islets (Fig. 5*B*). There was a significant reduction in insulin content per islet from *IRS-2*$^{-/-}$ mice compared with islets from wild-type mice (Fig. 5*C*). However, when normalized by cell number per islet, the insulin content in both genotypes was equivalent (Fig. 5*D*). In contrast, insulin secretion into the medium at high KCl (50 mmol/l) was slightly decreased in *IRS-2*$^{-/-}$ mice compared with wild-type mice (Fig. 5*E*). When normalized by the cell number per islet, high KCl-induced insulin secretion was equivalent in *IRS-2*$^{-/-}$ and wild-type mice (Fig. 5*F*).

Decreased insulin content and insulin secretion in *IRS-1*$^{-/-}$ mice. To investigate the role of IRS-1 in the function of individual β-cells, we next determined glucose-induced insulin secretion in *IRS-1*$^{-/-}$ mice by static incubation of the same numbers of islets for 1 h. Whereas insulin secretion into the medium by islets from *IRS-1*$^{-/-}$ and wild-type mice was similar at 2.8, 5.6, and 11.1 mmol/l glucose, at 22.2 mmol/l glucose, insulin secretion by islets from *IRS-1*$^{-/-}$ mice decreased slightly compared with islets from wild-type mice (Fig. 6*A*). When glucose-induced insulin secretion was normalized by cell number (although insulin secretion into the medium by islets from both *IRS-1*$^{-/-}$ and wild-type mice was similar at 2.8 and 5.6 mmol/l glucose), insulin secretion by islets from *IRS-1*$^{-/-}$ mice was slightly decreased at 11.1 mmol/l glucose and significantly decreased at 22.2 mmol/l glucose compared with islets from wild-type mice (Fig. 6*B*). Insulin content was slightly but significantly decreased in *IRS-1*$^{-/-}$ mice compared with wild-type mice (Fig. 6*C*). When normalized by cell number per islet, there was a more significant reduction in insulin content per islet from *IRS-1*$^{-/-}$ mice compared with wild-type mice (Fig. 6*D*).

DISCUSSION

IRS-2$^{-/-}$ mice were hyperinsulinemic and resistant to the glucose-lowering effect of insulin, strongly suggesting that *IRS-2*$^{-/-}$ mice were insulin resistant. However, whereas both *IRS-1*$^{-/-}$ and *IRS-2*$^{-/-}$ mice were insulin resistant, *IRS-1*$^{-/-}$ mice showed only minimally impaired glucose tolerance because hyperplasia of pancreatic β-cells compensated for insulin resistance (10). In marked contrast, *IRS-2*$^{-/-}$ mice failed to show compensatory hyperplasia of pancreatic β-cells, which appears to be the cause of the development of type 2 diabetes. Thus, a single gene mutation in this animal model was sufficient to induce both the peripheral insulin resistance and the β-cell defect seen in typical type 2 diabetes in humans (23), confirming the original report on *IRS-2*$^{-/-}$ mice (15).

The absence of IRS-2 appears to cause insulin resistance in the liver rather than the skeletal muscle, since insulin-stimulated PI 3–kinase activity associated with tyrosine-phosphorylated proteins was impaired in the liver but normal in the skeletal muscle of *IRS-2*$^{-/-}$ mice. These results are inconsistent with the original report of *IRS-2*$^{-/-}$ mice (15), in which it is argued that *IRS-2*$^{-/-}$ mice have insulin resistance in both liver and skeletal muscle, but are consistent with a more recent report from the same group (24). In contrast to *IRS-2*$^{-/-}$ mice, we and others previously reported that *IRS-1*$^{-/-}$ mice showed insulin resistance in the skeletal muscle but not in the liver (13,14). Thus, we would like to propose that IRS-1 plays a major role in the skeletal muscle and IRS-2 plays a major role in the liver in the regulation of insulin actions. Our data are consistent with the previous report that IRS-2 is required for insulin action in hepatocytes (25).

In contrast to the previously reported β-cell hyperplasia in *IRS-1*$^{-/-}$ mice (10), *IRS-2*$^{-/-}$ mice showed failure of compensatory β-cell hyperplasia in response to insulin resistance. Thus IRS-2, but not IRS-1, is required for compen-

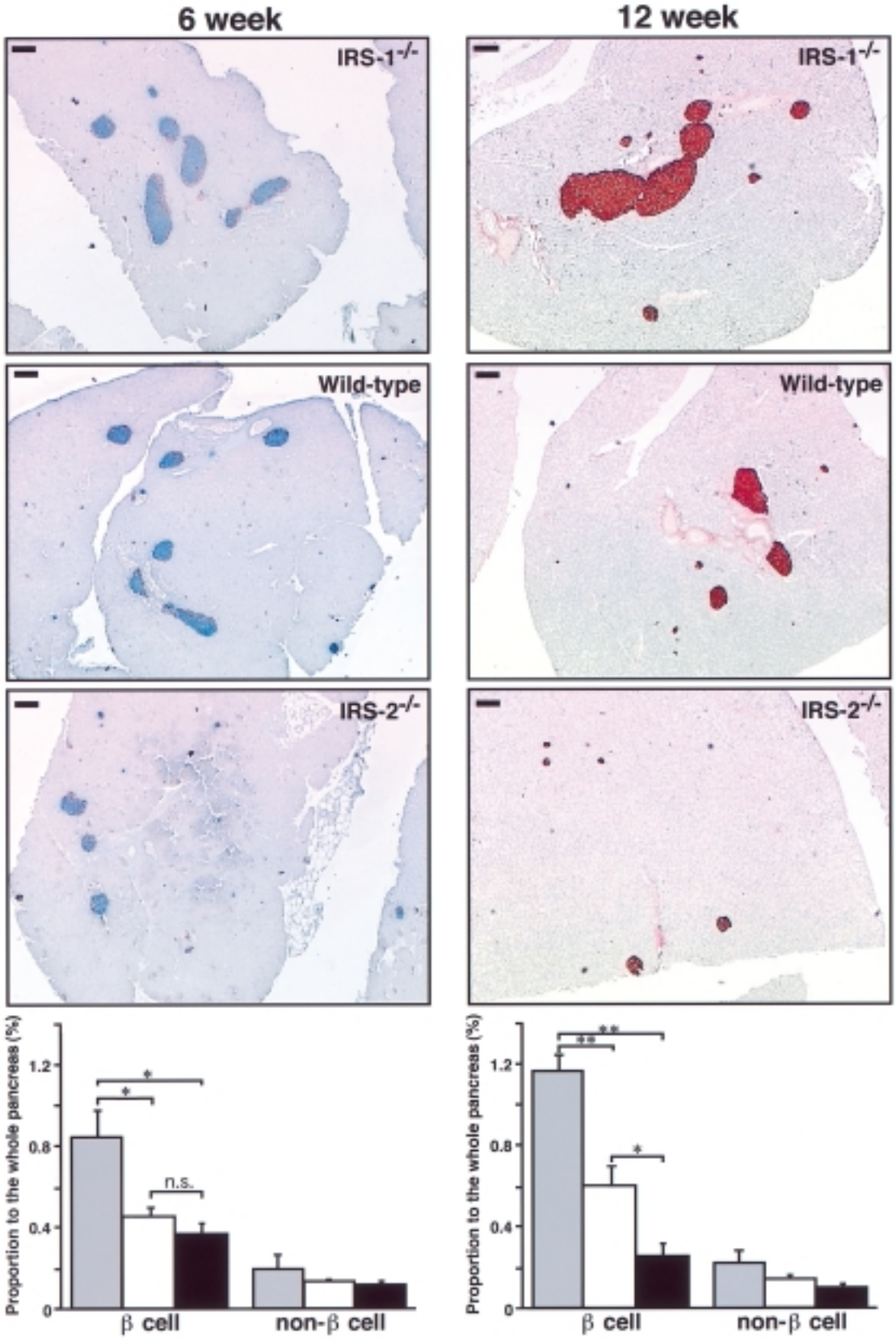

FIG. 4. Reduced β-cell mass in *IRS-2*$^{-/-}$ mice. Histological analysis of pancreatic islets and quantitation of β-cell mass in wild-type, *IRS-1*$^{-/-}$, and *IRS-2*$^{-/-}$ mice at 6 and 12 weeks. Pancreatic sections were double-stained with anti-insulin antibody and cocktails of anti-glucagon, anti-somatostatin, and anti-pancreatic polypeptide antibodies. Representative islets viewed on a computer monitor are shown. Bars indicate 100 μm. The area of the β-cells, the non–β-cells (α-cells plus δ-cells and PP cells), and the pancreas were calculated by computer-treated imaging. Results are shown as proportions of β-cell or non–β-cell area to the area of the pancreas (%) (mean ± SE, n = 4). ▒, *IRS-1*$^{-/-}$ mice; □, wild-type mice; ■, *IRS-2*$^{-/-}$ mice. *P < 0.05; **P < 0.01.

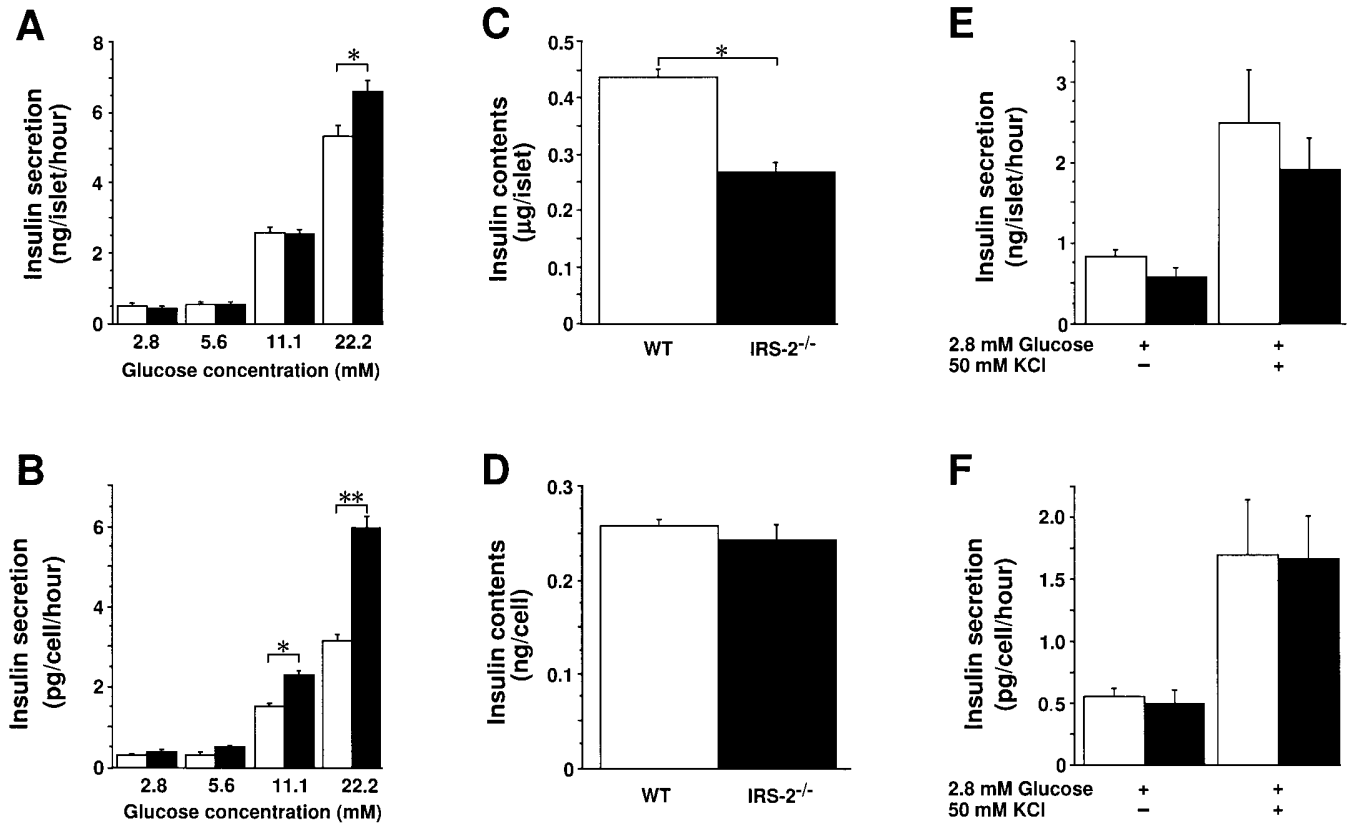

FIG. 5. Normal insulin content and increased insulin secretion in *IRS-2*$^{-/-}$ mice. *A*: Rates of insulin secretion per islet during static incubation of islets from wild-type and *IRS-2*$^{-/-}$ mice for 1 h at the glucose levels indicated. Values are expressed as means ± SE (n = 4). Similar results were obtained in two independent experiments. □, wild-type mice; ■, *IRS-2*$^{-/-}$ mice. *P < 0.05. *B*: Insulin secretion normalized by cell number per islet for wild-type and *IRS-2*$^{-/-}$ mice at the glucose levels indicated. Values are expressed as means ± SE (n = 4). Similar results were obtained in two independent experiments. *P < 0.05; **P < 0.01. *C*: Insulin content per islet of wild-type (WT) and *IRS-2*$^{-/-}$ mice. Values are expressed as means ± SE (n = 4). Similar results were obtained in more than three independent experiments. *P < 0.05. *D*: Insulin content normalized by cell number per islet in wild-type and *IRS-2*$^{-/-}$ mice. Values are expressed as means ± SE (n = 4). Similar results were obtained in more than three independent experiments. *E*: High KCl (50 mmol/l)-induced insulin secretion in wild-type and *IRS-2*$^{-/-}$ mice. *F*: Insulin secretion normalized by cell number per islet in wild-type and *IRS-2*$^{-/-}$ mice at high KCl. Values are expressed as means ± SE (n = 4).

satory β-cell hyperplasia in response to insulin resistance. In principle, a reduction in β-cell mass can be caused either by reduced β-cell differentiation/growth or increased β-cell death. White's group (26) has recently shown that IRS-2 deficiency in the islets was associated with increased β-cell apoptosis. The molecular basis for the different roles of IRS-1 and IRS-2 in the regulation of β-cell mass is presently unknown. It is possible that IRS-2 interacts more efficiently with IGF-1 receptor (26), insulin receptor–related receptor (27), or unidentified growth factor receptors other than IRS-1. Alternatively, the molecular basis for the different roles of IRS-1 and IRS-2 in the regulation of β-cell mass may relate to the levels of expression of IRS-1 and IRS-2 in β-cells.

In contrast to the defect in compensatory β-cell hyperplasia in *IRS-2*$^{-/-}$ mice, the function of individual β-cells from *IRS-2*$^{-/-}$ mice appeared to be supernormal. On the other hand, the function of individual β-cells from *IRS-1*$^{-/-}$ mice appeared to be impaired despite increased β-cell mass. Thus, IRS-1 and IRS-2 may also have different roles in glucose-induced insulin secretion from β-cells. This result may not be explained by the levels of expression of IRS-1 and IRS-2 in β-cells. As discussed above, it seems possible that IRS-2 interacts more efficiently with the IGF-1 receptor, and IRS-1 interacts more efficiently with the insulin receptor at β-cells. Rother et al. (25) have reported that IRS-2 interacts more efficiently with insulin receptors in hepatocytes. The kinetics of interaction between IRS-2 and insulin receptors or IGF-1 receptors may vary with the tissues. In fact, Kahn's group (28) reported that β-cell–specific insulin receptor knockout mice showed a defect in glucose-induced insulin secretion with normal β-cell mass, possibly via impaired tyrosine phosphorylation of IRS-1 but not of IRS-2. Moreover, IGF-1 has been reported to suppress glucose-induced insulin secretion from β-cells (29). This suppression of insulin secretion was caused by IGF-1–induced activation of PI 3-kinase and protein kinase B and phosphorylating and activating phosphodiesterase 3B, thereby reducing cAMP levels in the β-cells. Thus, it seems possible that defective activation of PI 3-kinase associated with IRS-2 in *IRS-2*$^{-/-}$ mice may be involved in supernormal insulin secretion in response to glucose.

A significant difference in the phenotypes of *IRS-2*$^{-/-}$ mice between our group and White's group (15) was seen in the severity of diabetes. Our *IRS-2*$^{-/-}$ mice had a fasting plasma glucose level of ~120 mg/dl at 10–20 weeks, which is clearly lower than the 350–400 mg/dl level seen at 16 weeks in their *IRS-2*$^{-/-}$ mice (15). This difference may reflect the severity of

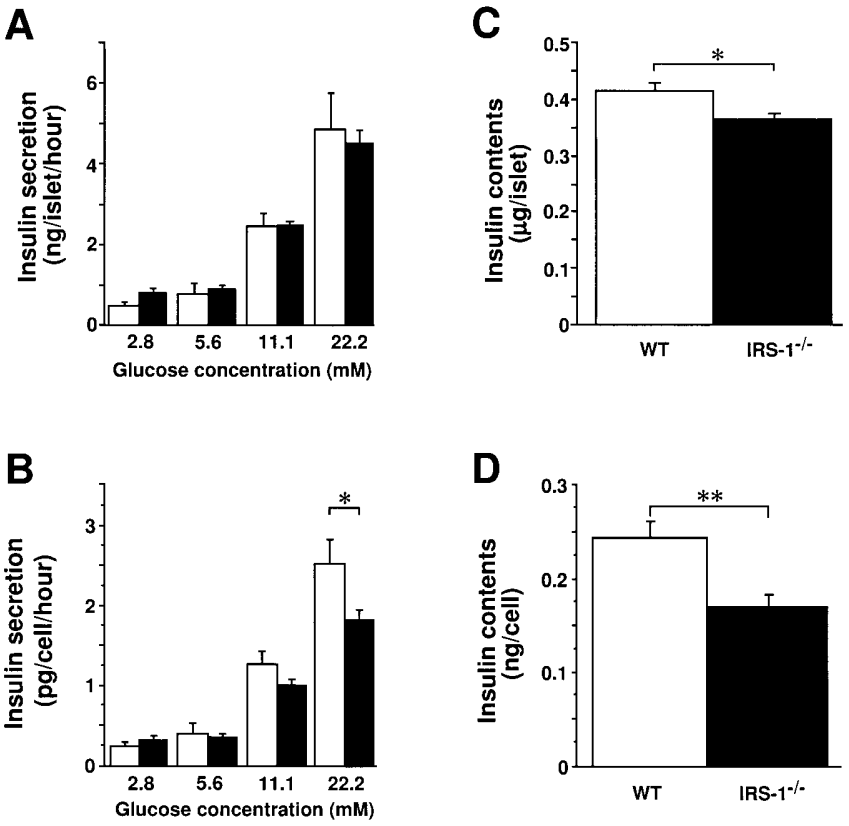

FIG. 6. Decreased insulin content and insulin secretion in *IRS-1*$^{-/-}$ mice. *A*: Rates of insulin secretion per islet during a static incubation of islets from wild-type and *IRS-1*$^{-/-}$ mice for 1 h at the glucose levels indicated. Values are expressed as means ± SE (n = 4). Similar results were obtained in more than three independent experiments. □, Wild-type mice; ■, *IRS-1*$^{-/-}$ mice. *B*: Insulin secretion normalized by cell number per islet in wild-type and *IRS-1*$^{-/-}$ mice at indicated glucose levels. Values are expressed as means ± SE (n = 4). Similar results were obtained in more than three independent experiments. *P < 0.05. *C*: Insulin content per islet of wild-type (WT) and *IRS-1*$^{-/-}$ mice. Values are expressed as means ± SE (n = 4). Similar results were obtained in more than three independent experiments. *P < 0.05. *D*: Insulin content normalized by cell number per islet in wild-type and *IRS-1*$^{-/-}$ mice. Values are expressed as means ± SE (n = 4). Similar results were obtained in more than three independent experiments. **P < 0.01.

reduction of the β-cell mass. In fact, the β-cell mass of our *IRS-2*$^{-/-}$ mice was reduced to 83% of that of the wild-type mice, and the reduction was milder than the 50% reduction in White's *IRS-2*$^{-/-}$ mice at 6 weeks (15). These differences may be due to genetic background (C57Bl/6 × CBA vs. C57Bl/6 × 129/Sv). In this respect, it should also be noted that these quantitative differences in *IRS-2*$^{-/-}$ mice may suggest the existence of some major modifier genes, as was previously reported in the *IR*$^{+/-}$*IRS-1*$^{+/-}$ mice (30).

We have previously shown that type 2 diabetes can be caused by the combination of insulin resistance due to homozygous inactivation of IRS-1 plus insulin deficiency due to heterozygous knockout of glucokinase (10). Although these double knockout mice developed compensatory hyperplasia of β-cells, the heterozygous defect in glucokinase impaired the ability of glucose to elicit insulin secretion. In contrast, *IRS-2*$^{-/-}$ mice develop type 2 diabetes because of failure of compensatory β-cell hyperplasia in response to insulin resistance, although the function of individual β-cells is normal or supernormal.

Thus, there are at least two molecular pathways in the development of type 2 diabetes. The first is failure of compensatory hyperinsulinemia in response to insulin resistance due to impaired β-cell function, as seen in heterozygous β-cell glucokinase/IRS-1 double knockout mice. The second is failure of compensatory hyperinsulinemia in response to insulin resistance due to impaired β-cell hyperplasia, as seen in *IRS-2*$^{-/-}$ mice. It is possible that both mechanisms may contribute to the development of human type 2 diabetes. Although a reduction in β-cell mass has been described in some patients with type 2 diabetes, it is possible that impaired function of individual β-cells may contribute to the pathogenesis of the disease in some patients.

ACKNOWLEDGMENTS

This work was supported by a Grant-in-Aid for Creative Basic Research (10NP0201) from the Ministry of Education, Science, Sports, and Culture of Japan (T.K.).

We thank Dr. Mitsuhiko Noda, Dr. Kazuo Hara, Katsuko Takasawa, Eri Yoshida-Nagata, Yuko Muto, Ayumi Nagano, and Hiroshi Chiyonobu for their excellent technical assistance and mouse husbandry.

REFERENCES

1. Kadowaki T: Insight into insulin resistance and type 2 diabetes from knockout mouse models. *J Clin Invest* 106:459–465, 2000
2. White MF, Maron R, Kahn CR: Insulin rapidly stimulates tyrosine phosphorylation of a Mr 185,000 protein in intact cells. *Nature* 318:183–186, 1985

3. Kadowaki T, Koyasu S, Nishida E, Tobe K, Izumi T, Takaku F, Sakai H, Yahara I, Kasuga M: Tyrosine phosphorylation of common and specific sets of cellular proteins rapidly induced by insulin, insulin-like growth factor-I and epidermal growth factor in KB cells. *J Biol Chem* 262:7342–7350, 1987
4. Shemer J, Ademo M, Wilson GL, Heffez D, Zick Y, LeRoith D: Insulin and insulin-like growth factor-1 stimulate a common endogenous phosphoprotein substrate (pp185) in intact neuroblastoma cells. *J Biol Chem* 262:15476–15482, 1987
5. Sun XJ, Wang LM, Zhang Y, Yenush L, Myers MG Jr, Glasheen E, Lane WS, Pierce JH, White MF: Role of IRS-2 in insulin and cytokine signalling. *Nature* 377:173–177, 1995
6. Lavan BE, Lane WS, Lienhard GE: The 60-kDa phosphotyrosine protein in insulin-treated adipocytes is a new member of the insulin receptor substrate family. *J Biol Chem* 272:11439–11443, 1997
7. Lavan BE, Fantin VR, Chang ET, Lane WS, Keller SR, Lienhard GE: A novel 160-kDa phosphotyrosine protein in insulin-treated embryonic kidney cells is a new member of the insulin receptor substrate family. *J Biol Chem* 272:21403–21407, 1997
8. Tamemoto H, Kadowaki T, Tobe K, Yagi T, Sakura H, Hayakawa T, Terauchi Y, Ueki K, Kaburagi Y, Satoh S, Sekihara H, Yoshioka S, Horikoshi H, Furuta Y, Ikawa Y, Kasuga M, Yazaki Y, Aizawa S: Insulin resistance and growth retardation in mice lacking insulin receptor substrate-1. *Nature* 372:182–186, 1994
9. Araki E, Lipes MA, Patti ME, Brüning JC, Haag IB, Johnson RS, Kahn CR: Alternative pathway of insulin signaling in mice with targeted disruption of the IRS-1 gene. *Nature* 372:186–190, 1994
10. Terauchi Y, Iwamoto K, Tamemoto H, Komeda K, Ishii C, Kanazawa Y, Asanuma N, Aizawa T, Akanuma Y, Yasuda K, Kodama T, Tobe K, Yazaki Y, Kadowaki T: Development of non-insulin-dependent diabetes mellitus in the double knockout mice with disruption of insulin receptor substrate-1 and β cell glucokinase genes: genetic reconstitution of diabetes as a polygenic disease. *J Clin Invest* 99:861–866, 1997
11. Patti ME, Sun XJ, Brüning JC, Araki E, Lipes MA, White MF, Kahn CR: 4PS/insulin receptor substrate (IRS)-2 is the alternative substrate of the insulin receptor in IRS-1-deficient mice. *J Biol Chem* 270:24670–24673, 1995
12. Tobe K, Tamemoto H, Yamauchi T, Aizawa S, Yazaki Y, Kadowaki T: Identification of a 190-kDa protein as a novel substrate for the insulin receptor kinase functionally similar to insulin receptor substrate-1. *J Biol Chem* 270: 5698–5701, 1995
13. Yamauchi T, Tobe K, Tamemoto H, Ueki K, Kaburagi Y, Yamamoto-Honda R, Takahashi Y, Yoshizawa F, Aizawa S, Akanuma Y, Sonenberg N, Yazaki Y, Kadowaki T: Insulin signalling and insulin actions in the muscles and livers of insulin-resistant insulin receptor substrate 1-deficient mice. *Mol Cell Biol* 16:3074–3084, 1996
14. Brüning JC, Winnay J, Cheatham B, Kahn RC: Differential signaling by insulin receptor substrate 1 (IRS-1) and IRS-2 in IRS-1-deficient cells. *Mol Cell Biol* 17:1513–1521, 1997
15. Withers DJ, Gutierrez JS, Towery H, Burks DJ, Ren JM, Previs S, Zhang Y, Bernal D, Pons S, Shulman GI, Bonner-Weir S, White MF: Disruption of IRS-2 causes type 2 diabetes in mice. *Nature* 391:900–904, 1998
16. Yagi T, Aizawa S, Tokunaga T, Shigetani Y, Takeda N, Ikawa Y: A role for Fyn tyrosine kinase in the suckling behavior of neonatal mice. *Nature* 366:742–745, 1993
17. Yagi T, Tokunaga T, Furuta Y, Nada S, Yoshida M, Tsukada T, Saga Y, Takeda N, Ikawa Y, Aizawa S: A novel cell line, TT2, with high germline-differentiating potency. *Anal Biochem* 214:70–76, 1993
18. Kubota N, Terauchi Y, Miki H, Tamemoto H, Yamauchi T, Komeda K, Nakano R, Ishii C, Sugiyama T, Eto K, Tsubamoto Y, Okuno A, Murakami K, Sekihara H, Hasegawa G, Naito M, Toyoshima Y, Tanaka S, Shiota K, Kitamura T, Fujita T, Ezaki O, Aizawa S, Nagai R, Tobe K, Kimura S, Kadowaki T: PPARγ mediates high-fat diet-induced adipocyte hypertrophy and insulin resistance. *Mol Cell* 4:597–609, 1999
19. Terauchi Y, Tsuji Y, Satoh S, Minoura H, Murakami K, Okuno A, Inukai K, Asano T, Kaburagi Y, Ueki K, Nakajima H, Hanafusa T, Matsuzawa Y, Sekihara H, Yin Y, Barrett JC, Oda H, Ishikawa T, Akanuma Y, Komuro I, Suzuki M, Yamamura K, Kodama T, Suzuki H, Koyasu S, Aizawa S, Tobe K, Fukui Y, Yazaki Y, Kadowaki T: Increased insulin sensitivity and hypoglycaemia in mice lacking the p85α subunit of phosphoinositide 3-kinase. *Nat Genet* 21:230–235, 1999
20. Ishii C, Kawazu S, Utsugi T, Ito Y, Ohno T, Kato N, Shimizu M, Tomono S, Nagai R, Komeda K: Beta-cell replication in insulin-induced remission of IDDM in BB/Wor/Tky rats. *Diabetes Res* 31:1–18, 1996
21. Eto K, Tsubamoto Y, Terauchi Y, Sugiyama T, Kishimoto T, Takahashi N, Yamauchi N, Kubota N, Murayama S, Aizawa T, Akanuma Y, Aizawa S, Kasai H, Yazaki Y, Kadowaki T: Role of NADH shuttle system in glucose-induced activation of mitochondrial metabolism and insulin secretion. *Science* 283:981–985, 1999
22. Eto K, Suga S, Wakui M, Tsubamoto Y, Terauchi Y, Taka J, Aizawa S, Noda M, Kimura S, Kasai H, Kadowaki T: NADH shuttle system regulates K_{ATP} channel-dependent pathway and steps distal to cytosolic Ca^{2+} concentration elevation in glucose-induced insulin secretion. *J Biol Chem* 274:25386–25392, 1999
23. Taylor SI, Accili D, Imai Y: Insulin resistance or insulin deficiency: which is the primary cause of NIDDM? *Diabetes* 43:735–740, 1994
24. Higaki Y, Wojtaszewski JF, Hirshman MF, Withers DJ, Towery H, White MF, Goodyear LJ: Insulin receptor substrate-2 is not necessary for insulin- and exercise-stimulated glucose transport in skeletal muscle. *J Biol Chem* 274:20791–20795, 1999
25. Rother KI, Imai Y, Caruso M, Beguinot F, Formisano P, Accili D: Evidence that IRS-2 phosphorylation is required for insulin action in hepatocytes. *J Biol Chem* 273:17491–17497, 1998
26. Withers DJ, Burks DJ, Towery HH, Altamuro SL, Flint CL, White MF: Irs-2 coordinates Igf-1 receptor-mediated beta-cell development and peripheral insulin signalling. *Nat Genet* 23:32–40, 1999
27. Hirayama I, Tamemoto H, Yokota H, Kubo SK, Wang J, Kuwano H, Nagamachi Y, Takeuchi T, Izumi T: Insulin receptor-related receptor is expressed in pancreatic beta-cells and stimulates tyrosine phosphorylation of insulin receptor substrate-1 and -2. *Diabetes* 48:1237–1244, 1999
28. Kulkarni RN, Brüning JC, Winnay JN, Postic C, Magnuson MA, Kahn CR: Tissue-specific knockout of the insulin receptor in pancreatic beta cells creates an insulin secretory defect similar to that in type 2 diabetes. *Cell* 96:329–339, 1999
29. Zhao AZ, Zhao H, Teague J, Fujimoto W, Beavo JA: Attenuation of insulin secretion by insulin-like growth factor 1 is mediated through activation of phosphodiesterase 3B. *Proc Natl Acad Sci U S A* 94:3223–3228, 1997
30. Brüning JC, Winnay J, Bonner-Weir S, Taylor SI, Accili D, Kahn CR: Development of a novel polygenic model of NIDDM in mice heterozygous for IR and IRS-1 null alleles. *Cell* 88:561–572, 1997